Supplementary Material

EXPERIMENTAL DATA

The full data measured for 82 TLSs is presented in Table I and the $T_1(S)$, $T_2(S)$ and $T_\phi(S)$ values are plotted in figure 1. Figure 1a contains 82 data points while 1b contains only 42. For about 50 % of the cases the dephasing time could not be determined, due to both low visibility and short dephasing time. This happens mostly for small splittings, which do not lie in the range of points presented in Fig. 3d of the main paper. For points that lie within this range and are omitted from the analysis we separately checked that the shorter coherence time does not affect the trend. The number of points in Fig. 1c is further reduced because for some T_1 limited TLSs we measured T_2 which is slightly longer than $2T_1$ due to measurement error. T_ϕ is excluded from the figure and table for these cases (three TLSs).

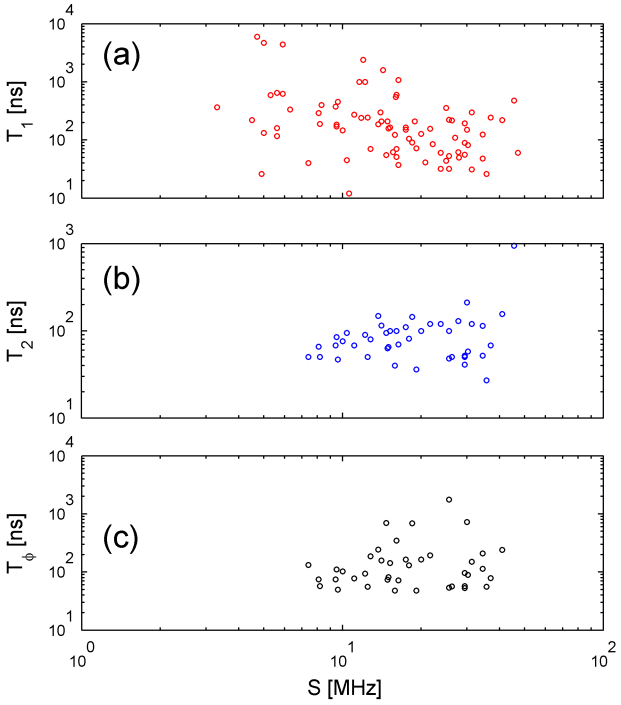

Figure 1: (a) Measured T_1 *vs.* splitting, (b) T_2 *vs.* splitting and (c) T_ϕ *vs.* splitting for all the measured TLSs. The spread in the T_1 data at a particular splitting value results from the random distribution of TLS orientation in the junction. It is apparent that the maximal lifetime shortens at larger splittings, consistent with dipole radiation. The spread of the T_2 data appears independent of the splitting, however the average values show some dependence which becomes more prominent in the dephasing times.

The errors in Fig. 3b and and Fig. 3c in the main paper represent the statistical spread of the data within a 7 MHz window. They are calculated by normalizing the standard deviation by $\sqrt{N}$, where N is the number of points within the window.

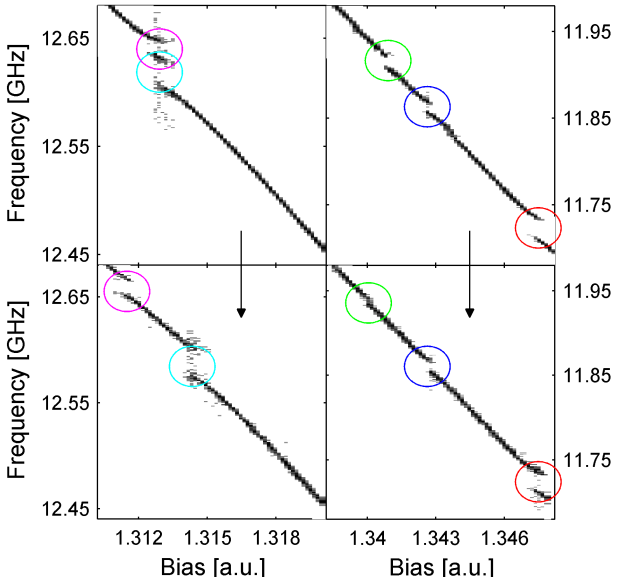

Figure 2: Qubit spectrum as a function of bias, before and after warmup to 1.5 K. Upper: two sections of the spectrum before warmup. Lower: the same sections, taken after heating the sample to 1.5 K and cooling down back to 10 mK. Circles with the same color indicate a splitting that we attribute to the same TLS. Both the position in frequency and splitting size of the TLSs are similar, indicating that the TLSs are not fully reset at this temperature.

We would like to point out that two points in Fig. 3c in the main paper have been excluded from the fit to a power law. These are the points with the largest average splittings (38 MHz and 46 MHz), where the statistics within each window is low (3 data points and 2 data points respectively). If we include these points in the fit we obtain an exponent $\alpha = -0.93$. We believe that the data points at the largest splittings may result from anomalous TLSs.

As pointed out in the main paper, some of the TLSs are changing in time. This is characterized by a change in the TLSs' transition energy, causing them to disappear from time to time (that is, to step out of our measurement bandwidth) or appear at a slightly different energy. An example of this phenomenon can be seen in Fig. 1 of the main paper. The leftmost TLS appears in the spectrum at larger bias value (that is smaller transition energy) than in the time-domain sweep. These two measurements were taken at an interval of one day.

New sets of TLSs are produced from the same device by

warming up to 20 K. We believe that some TLSs are not fully reset after warming up to only 1.5 K. Some splittings in the spectrum are similar in their frequency and splitting size to those before a partial warmup, as indicated in Fig. 2. Both the reset of TLSs at high temperatures, and the fact that some of the TLSs are changing in time indicate the true nature of the TLS as an approximation of a multilevel state, resulting from a multi-well energy structure.

STOCHASTIC SIMULATION

We reproduced the lifetime distribution of an ensemble of TLSs according to the TLS model in the following way. For each TLS we assume a uniform distribution of dipole orientation ($\cos\eta$ distributes uniformly, where η is angle relative to the electric field inside the junction), a potential asymmetry Δ from a uniform distribution ($\Delta \propto z$, where z is the effective distance between position states of the TLS inside the junction) and a tunneling energy Δ_0 from a log distribution ($\ln\Delta_0 \propto z$). These distributions are consistent with the TLS model, which assumes linear sensitivity of Δ on z and exponential sensitivity of Δ_0 on z. We excluded TLSs having smaller couplings than we can measure. For each TLS we compute the lifetime according to Eq. 1 in the main paper ($T_1(\sin(\theta)) = a/\sin(\theta)^2$, where $\theta = \arctan(\Delta_0/\Delta)$ and a is some constant). The simulation data points were then averaged over a 7 MHz window size, as done for the experimental data.

The resulting $\langle T_1(S)\rangle$ behavior (see Fig. 3c in the main paper, blue diamonds) resembles a sum of two power laws. At smaller splittings $S \lesssim S_{max}/2$, the points fit a power law with an exponent $\alpha_1 \approx -1.9$, while for larger splittings they fit a power law with an exponent $\alpha_2 \approx -1$. A similar trend is observed in our data as well.

f_{ge} [GHz]	S [MHz]	T_1 [ns]	T_2 [ns]	T_ϕ [ns]	CD No.
12.8	3.3	365	-	-	6
11.43	4.5	220	-	-	3
11.35	4.7	6000	-	-	7
12.45	4.9	26	-	-	7
11.55	5.0	4700	-	-	4
11.31	5.0	132	-	-	7
11.23	5.3	590	-	-	4
11.462	5.6	650	-	-	3
13.08	5.6	117	-	-	4
11.33	5.6	160	-	-	4
12.89	5.9	4400	-	-	6
11.4	5.9	623	-	-	6
12.79	6.3	335	-	-	4
13.11	7.4	40	50	133	4
12.85	8.1	291	66	74	3
12.13	8.2	190	50	58	5
11.57	8.3	400	-	-	4
11.45	9.4	373	68	75	5
11.835	9.5	170	-	-	2
11.342	9.5	185	85	110	2
12.26	9.6	453	47	50	2
12.32	10.0	147	76	102	5
11.85	10.4	45	95	-	4
11.6	10.6	12	-	-	6
12.25	11.1	275	68	78	7
12	11.6	1000	-	-	4
11.86	11.8	240	-	-	2
11.22	12.0	2400	-	-	1
11.88	12.2	1000	90	94	5
12.57	12.5	243	50	56	6
11.96	12.8	70	80	187	3
11.515	13.7	187	148	245	2
11.96	14.0	300	-	-	4
10.96	14.1	209	115	159	2
10.8	14.3	1600	-	-	7
13.22	14.7	55	95	697	6
11.57	14.9	210	63	74	3
11.27	15.0	158	65	82	5
12.24	15.2	165	100	143	3
11.7	15.6	62	-	-	4
11.38	15.9	123	40	48	7
11.59	16.0	550	-	-	7
11.78	16.1	51	-	-	5
11.62	16.1	70	100	350	5
10.95	16.1	600	-	-	1
12.642	16.4	1080	70	72	2
11.85	16.4	37	-	-	7
12.41	17.5	165	110	165	5
12.37	17.5	150	-	-	7
12.542	18.0	106	81	131	8
11.42	18.5	91	144	690	4
11.915	18.9	208	-	-	2
12.47	19.2	72	36	48	6
11.21	20.0	127	100	165	5
12.73	20.8	41	-	-	7
11.86	21.7	156	120	195	2
12.15	22.2	85	-	-	7
11.72	23.8	60	120	-	2
12.66	23.8	32	-	-	7
12.44	25.0	44	-	-	6
11.86	25.0	355	-	-	1
11.61	25.6	53	100	1767	3
12.34	25.6	32	-	-	6
11.73	25.6	224	48	54	7
13.04	26.3	217	50	57	6
12.675	27.0	110	-	-	1
11.77	27.8	62	130	2687	4
12.2	28.0	50	-	-	1
12.613	29.4	56	52	97	2
11.22	29.4	89	41	53	2
12.67	29.4	193	50	57	3
12.147	30.0	150	212	723	8
12.34	30.3	82	58	90	4
11.89	31.3	31	-	-	6
10.91	31.3	300	120	150	7
12.78	34.5	125	114	210	5
12.12	34.5	48	52	113	6
11.59	35.7	26	27	56	2
11.17	37.0	243	68	79	6
11.772	41.0	220	156	242	1
12.05	45.5	476	950	-	4
11.99	47.0	60	-	-	1

Table I: Full measurement data of TLSs: TLS energy (f_{ge}), splitting (S), lifetime (T_1), coherence time (T_2) calculated dephasing time (T_ϕ) and cooldown number. The last column indicates which TLSs were measured on the same cooldown (i.e., temperature was not raised to more than 20 mK between measurements of TLSs belonging to the same cooldown).